New Journal of Physics
The open access journal at the forefront of physics

Deutsche Physikalische Gesellschaft DPG
IOP Institute of Physics

Published in partnership with: Deutsche Physikalische Gesellschaft and the Institute of Physics

OPEN ACCESS

RECEIVED
22 August 2021

REVISED
11 November 2021

ACCEPTED FOR PUBLICATION
22 November 2021

PUBLISHED
16 December 2021

PAPER

Quantum state tomography as a numerical optimization problem

Violeta N Ivanova-Rohling[1,2,3,*], **Guido Burkard**[1] and **Niklas Rohling**[1]

[1] Department of Physics, University of Konstanz, D-78457 Konstanz, Germany
[2] Zukunftskolleg, University of Konstanz, D-78457 Konstanz, Germany
[3] Department of Mathematical Foundations of Computer Sciences, Institute of Mathematics and Informatics, Bulgarian Academy of Sciences, Akad. G. Bonchev, Block 8, 1113 Sofia, Bulgaria
[*] Author to whom any correspondence should be addressed.

E-mail: violeta.ivanova-rohling@uni-konstanz.de, guido.burkard@uni-konstanz.de and niklas.rohling@uni-konstanz.de

Keywords: quantum state tomography, Grassmannian manifolds, orthoplex-bound-achieving set, mutually unbiased subspaces, NV centers in diamond, numerical optimization

Abstract

We present a framework that formulates the quest for the most efficient quantum state tomography (QST) measurement set as an optimization problem which can be solved numerically, where the optimization goal is the maximization of the information gain. This approach can be applied to a broad spectrum of relevant setups including measurements restricted to a subsystem. To illustrate the power of this method we present results for the six-dimensional Hilbert space constituted by a qubit–qutrit system, which could be realized e.g. by the ^{14}N nuclear spin-1 and two electronic spin states of a nitrogen-vacancy center in diamond. Measurements of the qubit subsystem are expressed by projectors of rank three, i.e. projectors on half-dimensional subspaces. For systems consisting only of qubits, it was shown analytically that a set of projectors on half-dimensional subspaces can be arranged in an informationally optimal fashion for QST, thus forming so-called mutually unbiased subspaces. Our method goes beyond qubits-only systems and we find that in dimension six such a set of mutually-unbiased subspaces can be approximated with a deviation irrelevant for practical applications.

1. Introduction

There has been a strong interest in quantum computing since the publication of Shor's algorithm [1] for prime factorization. Among other tasks performed efficiently by quantum computers are quantum simulations [2], aiming at finding the state of a system which is described by quantum mechanics or to compute its time evolution. Many physical platforms have been suggested for building a quantum computer, including trapped ions [3], superconducting qubits comprising Josephson junctions [4, 5], electron spins in semiconductor quantum dots [6, 7], and electron or nuclear spins at a nitrogen-vacancy (NV) defect in diamond [8]. However, despite impressive results regarding the coherent control and coupling of qubits, the implementation of a general purpose quantum computer with a number of qubits relevant for practical applications remains a challenge.

Any physical system which is supposed to function as a building block of a quantum computer would require tests of its functionality. The measurements and computations which allow the estimation of a quantum state are called quantum state tomography (QST) [9]. Alongside methods to characterize quantum processes, such as quantum process tomography, randomized benchmarking (RB) [10, 11], and gate set tomography [11–14], QST is part of the emerging field of quantum characterization, verification, and validation (QCVV), which is dedicated to the above mentioned tests of quantum systems. QST is a central tool for verifying and debugging a quantum device and can be helpful for the process of implementation of a quantum computer in a physical system. It allows for checking of the initialization of the quantum device and—as a building block of quantum process tomography—also the quantum gates.

Therefore, the scaling of QST is not only relevant for characterizing the initialization procedure within quantum computing but also for testing quantum gates. Specifically, quantum process tomography can be done by performing QST many times with different initial states [15] or even by QST with one initial state by using an ancillary system [16, 17]. The QST procedure calls for the acquisition of the full information of a quantum state, which requires numerous repetitions of a set of measurements and is typically very time-consuming. For situations where specific symmetries of the quantum state are known, the number of parameters which need to be determined can be reduced, e.g. for permutationally invariant tomography [18]. Other QCVV methods like low-rank tomography [19] or RB [20] while allowing to extract full information of a quantum state or a quantum process in limiting cases are designed for and typically applied to situations where prior knowledge of a quantum state or a quantum process is available. In contrast to that QST and quantum process tomography aim at determining unknown quantum states or processes without prior knowledge available, i.e. QST and quantum process tomography are complex procedures for gaining comprehensive information.

Because full QST is such a time consuming task, finding the most efficient QST measurement set is thus of high practical relevance. Note that analytical solutions to this problem are only known in a few cases, as we will see in the following discussion. Here, *most efficient* is used in terms of largest average information gain for a fixed number of experimental runs of each element of the QST measurement set, see section 2. For a minimal set of non-degenerate measurements, this problem was considered by Wootters and Fields [21]. For an n-dimensional Hilbert space, the ideal choice is a set of $n+1$ measurement operators whose eigenbases are mutually unbiased bases (MUBs) [21]. Improvements to QST using MUBs are possible by allowing (i) for more than the minimum number of measurements [22], (ii) for generalized measurements using ancillary systems yielding symmetric, informationally complete positive operator-valued measures (SIC-POVMs) as optimal measurements [23, 24], and (iii) for adjusting the choice of measurements on the run [25–27]. Wootters and Fields [21] introduced a geometric quality measure to evaluate the QST measurement set. It is important to note that the use of this quality measure is not limited to non-degenerate measurements. We have already applied this measure in the scenario where the measurements distinguish one state from the remaining $(n-1)$-dimensional subspace [28, 29]. These measurements are described as independent rank-1 projectors. The states can be chosen such that they belong to a set of MUBs [28], but a numerically optimized set of measurements outperforms the MUBs [29]. Furthermore, the geometric quality measure is not limited to rank-1 projection operators; on the contrary, we use it in this paper to evaluate a quorum of projection operators of higher rank.

We describe a general framework to formulate the search for an optimal QST measurement scheme as an optimization problem and use numerical methods to solve it. To illustrate the power of this method, this paper examines the settings where only a part of a composite system is accessible to direct measurements. The relevance of this scenario becomes clear when considering the following quantum computer architecture. One logical qubit is realized by a set of physical qubits and only one of the physical qubits is equipped with a measurement device. This can save resources on the hardware level compared to a system where each physical qubit is assigned its own measurement device. For a quantum algorithm to be performed, reading out one physical qubit out of the set of physical qubits which constitute the logical qubit is sufficient. However, the ancilla physical qubits are needed for quantum error correction. We have to require that universal quantum gates are available, i.e. any unitary operation can be performed in the Hilbert space describing this quantum system. The reasons for this are that universal quantum gates are needed for a general-purpose quantum computer as well as for realizing different measurements in the tomography scheme considered in this paper as we describe in the following. Results for optimal QST by measuring one out of several qubits are already available [30]. Therefore, we consider here the simplest composite system which does not consist only of qubits, i.e. a qubit–qutrit system, see figure 1. We describe the realization of such a system—in NV centers in diamond. We reveal the relation between our optimization problem of finding the optimal QST measurement set and packing problems in Grassmannian manifolds, which have been studied in great detail [30–40] and are relevant for many fields, such as wireless communication, coding theory, and machine learning [39, 41–44]. As we are able to approximate the optimal measurement scheme of the qubit–qutrit system, we solve a greater problem, namely we find a close approximation to an optimal Grassmannian packing of half-dimensional subspaces in Hilbert space of dimension six.

2. Our general framework for QST optimization

Now we present our general framework for finding an optimal QST measurement scheme for a user-specified system of finite dimension n, by solving a corresponding optimization problem. In figure 2, the framework of customized QST is visualized: the user interface consisting of input measurement

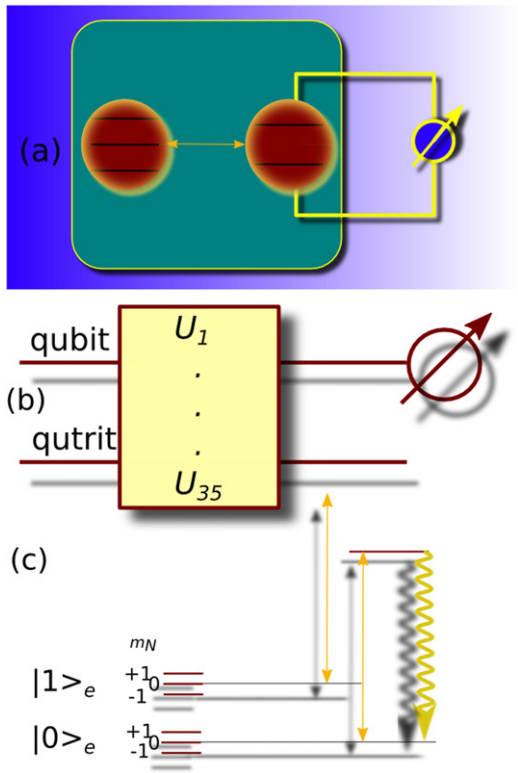

Figure 1. (a) Measurement setup for a qubit–qutrit system: only the qubit is measured, all unitary operations on the system including entangling gates between the qubit and the qutrit are available. (b) Quantum circuit of the measurement procedure: each of the 35 rank-3 projectors needed for a QST quorum are realized by applying a unitary operation U_j and then performing a projective measurement on the qubit to distinguish between the qubit states $|0\rangle$ and $|1\rangle$. The resulting projection operators are then given by $P_j = U_j |0\rangle \langle 0| \otimes 1_3 U_j^\dagger$ where 1_3 is the unity operation for the qutrit. Note that $U_1 = 1$. (c) The projection on the qubit state $|0\rangle$ can be realized for an electronic state in an NV center in diamond by resonance fluorescence where only the electronic state $|0\rangle_e$ is excited by radiation and leads to fluorescence, thus allowing for the read-out of the electronic state in the basis $\{|0\rangle_e, |1\rangle_e\}$. The state of the nuclear spin, m_N, is not measured directly.

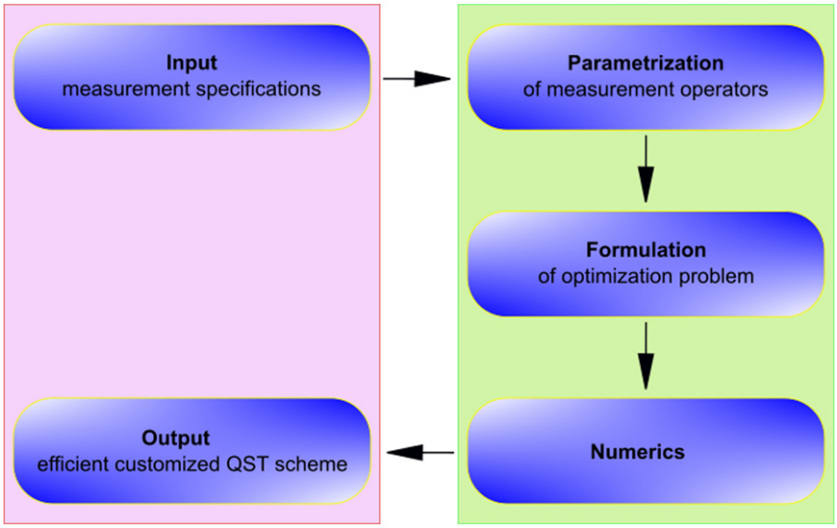

Figure 2. Workflow of the customized QST framework: on the left (red rectangle) is the user interface; on the right (green rectangle) are the internal process modules.

specifications and an efficient customized QST scheme as the output is abstracted away from the internal computational modules. Importantly, this procedure is quite flexible and allows to include case-specific constraints to the available measurement.

The input is formed by the specifications and restrictions of the available measurements for the quantum system under investigation. An important example of a restriction to measurement operators is

the specific rank of the projectors, e.g. reference [29] considers two-outcome measurements where the outcomes correspond to a rank-1 projector or to a rank-$(n-1)$ projector, respectively. Importantly, the situation where only a subsystem of the quantum system is measured can be described by a restriction on the ranks of the projection operators. Namely, the ranks of projection operators corresponding to this measurement are at least the dimension of the subsystem's complement. In this paper, we investigate in detail the restriction to measuring one qubit as part of a composite system yielding measurements described by projectors of rank $n/2$.

After the specifications of the system of interest are formulated, we parametrize the measurement operators such that the parameters determine the states in Hilbert space which span the subspace, corresponding to the projection operators. This allows us to use a minimal number of parameters for each projector and thus minimizes the dimension of the optimization problem.

In our framework, we adopt the geometric quality measure, as defined by Wootters and Fields [21], based on the information gain from the measurement results,

$$I = -\ln\left(\frac{V}{V_0}\right) + \text{const.} \tag{1}$$

where V_0 is the volume of the space of all possible density matrices and V is the confidence volume, which we will define more precisely in the following. The probability distribution after the measurement is assumed to be Gaussian. We consider the part of this Gaussian distribution which is at least $1/e$ times its maximum value. This part has an ellipsoidal shape. Now, the confidence volume V is the smallest rectangular volume enclosing this ellipsoid. Note that the factor $1/e$ is an arbitrary choice. When choosing a different number between zero and one, while changing the volume V and at the same time the constant in equation (1), neither the information gain nor the quality measure, which we will define below, is affected by this choice. For a set of measurement operators $\{M_j\}$, each measurement operator can be represented in its spectral decomposition, i.e. as the sum of its eigenvalues λ_{jk} times the projectors P_{jk} onto the respective eigenspaces, $M_j = \sum_k \lambda_{jk} P_{jk}$. Then, the quality measure $\mathcal{Q}$ is defined as the volume spanned in operator space by the traceless parts of the projectors. We will see soon the relation of $\mathcal{Q}$ to the confidence volume V. Wootters and Fields [21] considered the case of non-degenerate measurements where each measurement is represented by n rank-1 projection operators projecting on the eigenstates of the measurement operator. As the eigenvectors of one measurement operator form an orthogonal basis, the optimization problem lies in optimizing the relation between the different measurement operators or—in other words—between their eigenbases. The confidence volume V is given by [21]

$$V = \frac{V_1 \ldots V_{n+1}}{\mathcal{Q}} \quad \text{with } V_j \sim \frac{\sqrt{p_{j1} \cdots p_{jn}}}{(N_j)^{(n-1)/2}}, \tag{2}$$

where $p_{jk} = \mathrm{tr}(P_{jk}\rho)$ and N_j is the number of repetitions of the measurement j. Here, V_j is the confidence volume for the part of the density distribution for measurement j and using the same factor $1/e$ as above. The measurement outcome follows a multinomial distribution which can be approximated by a Gaussian for a large number of repetitions. This also justifies the previously mentioned assumption that the overall distribution after the measurements are performed is Gaussian. Averaging over the space of all density matrices removes the dependence on the p_{jk} and, under the assumption that each measurement is repeated the same number of times $N_{\mathrm{rep}} := N_1 = \cdots = N_{n+1}$, yields

$$\langle I \rangle = \ln(\mathcal{Q}) + \frac{n^2-1}{2}\ln(N_{\mathrm{rep}}) + \text{const.} \tag{3}$$

In the case considered in [29], the optimization problem is to arrange independent rank-1 projectors P_j maximizing the geometric quality measure. The extension of Wootters' and Fields' formalism is straightforward, just the expression for the confidence volume is changed to $V = \prod_{j=1}^{n^2-1} L_j/\mathcal{Q}$ with $L_j \sim \sqrt{p_j(1-p_j)/N_j}$ where $p_j = \mathrm{tr}(P_j\rho)$. Here, we extend the use of the quality measure $\mathcal{Q}$ to degenerate measurements where the measurement operators are denoted by projection operators which can be of rank higher than one. This is relevant for situations where a subsystem is measured rather than the full system. Further below, we will focus on measurements represented by projectors on half-dimensional subspaces. However, the approach could also easily cover other cases, e.g. measuring the qutrit in a qubit–qutrit system, where each measurement is described by three rank-2 projectors, two of which are independent. We use the geometric measure detailed above in the formulation of our optimisation problem. Note that all two-outcome measurements including the rank-1 case considered in [29] and the situation considered in this paper have in common that one measurement determines one parameter because by repeating the measurement two frequencies for the two possible outcomes are obtained. The two frequencies

(probabilities) depend on each other as they have to add up to one. Consequently, a QST measurement set consists of at least $n^2 - 1$ different measurements because the density matrix is given by $n^2 - 1$ real parameters. Then the confidence volume is—also in this more general case—given by $V = \prod_{j=1}^{n^2-1} L_j/\mathcal{Q}$ and again we have $L_j \sim \sqrt{p_j(1-p_j)/N_j}$ following from the underlying binomial distribution. Then, it follows straightforwardly that the expression for the averaged information gain is still of the form equation (3). The constant in that expression, however, depends on the rank of the projectors and is different for the non-degenerate case compared to the two-outcome measurements. However, this is unimportant for our optimization problem. The *length* of a projection operator of rank l in operator space is given by $\sqrt{\mathrm{tr}(P^2)} = \sqrt{l}$. Nevertheless, the volume spanned by the $n^2 - 1$ projectors is the correct quality measure for all ranks l following from the above considerations. Rescaling to unit vectors in operator space would be in principle possible by changing again the constant in equation (3). However, we will keep the length unchanged and instead compare to the upper bound of $\mathcal{Q}$ which would be reached if the traceless parts of the P_j form a hypercube. A formal description for the specific example solved in this paper is provided below.

We then tackle this problem by numerical means. The optimization problem of maximizing the volume spanned by the projection operators is a non-convex optimization problem. In order to explore the search space and find the global optimum, we used a combination of standard numerical methods, which for this problem was sufficient. More details on the methodology will be given below. For larger systems, the problem of finding optimal measurement schemes calls for more sophisticated approaches, such as ones based on machine learning and deep learning.

The output of our framework is a set of measurement operations, determined by the system's specifications and restrictions which have been given as input. This set of measurements allows the user to perform the most efficient state tomography procedure possible. This means the QST measurement set suggested by our optimization scheme maximizes average information gain for a fixed number of repetitions N_{rep} of each of the measurements. At the same time, if we aim at a certain fixed value for the information gain, then N_{rep} is minimized, see equation (3). Note that we limit the search to QST measurement sets with the minimal number of different measurements (quorum).

3. QST by measuring a qubit in a composite system

Despite the limitation of measuring no more than one qubit in each run, complete state tomography is possible if we combine the available measurement with unitary transformations. We ask what is the ideal choice of a minimal measurement set (quorum) for QST. If one out of N qubits is measured, a complete set of MUBs can be harnessed to construct an ideal quorum in the sense that the traceless parts of the rank-2^{N-1} projectors form a hypercube [30]. Then the geometric quality measure reaches its upper bound. For two qubits, QST with parity readout, a scenario equivalent to measuring one of the qubits, was proposed [46] and implemented [47] for spin qubits in quantum dots.

For a Hilbert space of (non-prime power) dimension six, which corresponds to the qubit–qutrit system we consider in this paper, a complete set of MUBs is not available. The goal of this paper is to show that a quorum of projectors can come so close to the upper bound for the geometric quality measure described above that the deviation is without practical relevance for performing QST. This is of practical importance because qubit–qutrit systems are among the experimentally studied quantum devices, as we will show below using a physical example. Moreover, our result has implications for Grassmannian packing problems, as we will discuss in detail in sections 4 and 5. Note that the work by Bodmann and Haas [30] is of frame-theoretical nature and the implication for QST is rather a corollary. In the same way our numerical result has implications for frame theory.

Formally, the problem we are solving is to find unitary operations $U_j (j = 1, \ldots, 35)$ acting on the six-dimensional Hilbert space such that the projection operators

$$P_j = U_j^\dagger \left|0\right\rangle \left\langle 0\right| \otimes 1_3 U_j \tag{4}$$

maximize $\mathcal{Q}$. Here, $\left|0\right\rangle \left\langle 0\right|$ is the projector on the ground state of the qubit and 1_3 is the identity operator for the qutrit. Also see figure 1(b).

An example for a qubit–qutrit system is a negatively charged NV center in diamond [48, 49]. If the nitrogen nucleus is a ^{14}N, then the nuclear spin is one, i.e. it represents a qutrit. Two states of the electronic spin-1 of the NV center effectively constitute a qubit. NV centers have been under intense investigation due to the long spin lifetimes of both, the nuclear spin and the electron state, and due to the possibility to perform unitary operations by microwave driving or by selectively exciting optical transitions between the energy levels of this quantum system [48]. Single-shot projective measurements on the lowest electronic

state can be done by resonant excitation fluorescence [49–52]. Such measurements can be described by rank-3 projectors which are considered here (see figure 1).

4. Packings in a Grassmannian manifold

The subspaces of dimension l described by the projection operators of rank l form a vector space with special properties, called a *Grassmannian manifold*. We will define this notion below. Given an n-dimensional vector space $\mathbb{V}$ over a field $\mathbb{F}$, a Grassmannian $\mathrm{Gr}(l, \mathbb{V})$ is the space of l-dimensional linear subspaces of $\mathbb{V}$. Subspace packing in a Grassmannian manifold, or *Grassmannian packing*, is the problem of maximizing the minimum pairwise distance in a set of subspaces. We will describe below in detail how this packing problem relates to the problem of optimal QST in the setting considered here. We consider the case in which $\mathbb{F} = \mathbb{C}$ and $\mathbb{V} = \mathbb{C}^6$. The problem of arranging a set of m subspaces $\{U_j \in \mathrm{Gr}(l, \mathbb{F}^n), j = 1, \ldots, m\}$ in an optimal, maximally spread fashion has been studied for both $\mathbb{F} = \mathbb{R}$ and $\mathbb{F} = \mathbb{C}$ [30–40]. Typically, optimality here refers to maximizing the minimum chordal distance $d_c^2(P_j, P_i) = l - \mathrm{tr}(P_j^\dagger P_i)$ where P_j is the projector on the subspace U_j, i.e. $\min_{i \neq j} d_c^2(P_j, P_i)$ shall be maximal.

Here we consider a problem which is different from optimal spreading, as we are not interested in maximizing the smallest distance between the projectors on the subspaces but in the subspaces being informationally independent. However, for the specific situation we consider, $\mathbb{F} = \mathbb{C}$, $l = n/2$, the optimal solutions for QST can be naturally extended to a maximum set of an optimal Grassmannian packing as we will discuss in the following.

5. Optimality condition, upper bound, and consequences

We consider a Hilbert space of dimension n and projection operators projecting onto subspaces of dimension l, later we will specialize to $n = 6$ and $l = 3$. Then, the measurements are described by rank-l projection operators. The matrix corresponding to a rank-l projection operator has l linearly independent columns, which define an l-dimensional subspace. Conversely, every l-dimensional subspace can be described by a projection operator of rank l.

A minimal state tomography set consists of $n^2 - 1$ of those projectors, $\{P_1, \ldots, P_{n^2-1}\}$. In this case, the problem of finding an optimal QST quorum is equivalent to the problem of arranging the projectors $P_j (j = 1, \ldots, n^2 - 1)$ in an optimal fashion. We define the traceless parts of these operators $Q_j = P_j - l\mathbb{1}/n$. As stated above, we evaluate the quorum by using the quality measure $\mathcal{Q}$ introduced by Wootters and Fields [21], defined as the volume spanned by $\{Q_1, \ldots, Q_{n^2-1}\}$ in the vector space of traceless $n \times n$ matrices with the scalar product $\mathrm{tr}(A^\dagger B)$. The length of the Q_j in this vector space is fixed to

$$\sqrt{\mathrm{tr}(Q_j^\dagger Q_j)} = \sqrt{\mathrm{tr}\left(\left(P_j - \frac{l\mathbb{1}}{n}\right)^\dagger \left(P_j - \frac{l\mathbb{1}}{n}\right)\right)} = \sqrt{l - \frac{l^2}{n}}, \tag{5}$$

and thus, the volume is fully determined by the angles between the Q_j.

An upper bound for the quality measure is

$$\mathcal{Q}_{\mathrm{ub}} = \left(l(1 - l/n)\right)^{(n^2-1)/2}, \tag{6}$$

which is reached only if $\mathrm{tr}(Q_j^\dagger Q_i) = 0$ for all $i \neq j$. Note that any rank-l projector is available since we assume that it is possible to perform one basic measurement projecting on an l-dimensional subspace and that all unitary operations can be performed. Below we describe how an upper-bound-reaching set of rank-$n/2$ projection operators relates to two other notions, namely mutually unbiased subspaces and quantum 2-designs.

5.1. Mutually unbiased subspaces

We want to see how reaching the upper bound compares to the chordal distance and find for $\mathrm{tr}(Q_j^\dagger Q_i) = 0$,

$$d_c^2(P_j, P_i) = \frac{l(n - l)}{n}. \tag{7}$$

This is the so-called orthoplex bound, which appears as an upper bound for the minimal chordal distance of projectors on l-dimensional subspaces in $\mathbb{C}^n$ for a set of at least $n^2 + 1$ elements [30]. If for two subspaces of the Hilbert space the corresponding projectors fulfill equation (7), they are called *mutually unbiased subspaces* [53]. Now, we will focus on the case $l = n/2$, i.e. the problem of packing of *half-dimensional*

subspaces. For this case, Bodmann and Haas [30] showed using a construction from a complete set of MUBs that if n is a power of two, an optimal orthoplex-bound-achieving packing, maximal in terms of the number of its elements, exists. This packing consists of n^2-1 projectors P_j whose corresponding Q_j are pairwise orthogonal, and the projectors $P_{j+n^2-1} = 1 - P_j$ for $j = 1, \ldots, n^2-1$. The maximal number of elements of a set of projectors which achieves the orthoplex bound is $2(n^2-1)$, thus this maximum of elements is reached here. In general—not limited to the case of n being a power of two—for $l = n/2$, the bound simplifies to $\mathcal{Q}_{\mathrm{ub}} = (n/4)^{(n^2-1)/2}$ and the condition for the pairwise chordal distance becomes

$$d_{\mathrm{c}}^2(P_j, P_i) = \frac{n}{4}. \tag{8}$$

For the qubit–qutrit system considered here, $n = 6$, and a quorum has 35 elements, and with $l = n/2 = 3$, the quality measure's upper bound is given by $\mathcal{Q}_{\mathrm{ub}} = (3/2)^{35/2} \approx 1206.69$. Note that the construction by Bodmann and Haas to obtain a maximal orthoplex-bound achieving set does not work in dimension six. Thus our numerical result contains novel insights in the existence of an (approximated) orthoplex bound achieving set and potential inspiration for numerically tackling the problem for higher dimensions which are not powers of two, such as ten or twelve.

5.2. Quantum 2-designs

The problem of optimal arrangement of projections is closely related to the notion of *quantum t-designs*. Furthermore, quantum t-designs are known to be highly relevant to optimal QST measurement schemes. For the situation of measuring a qubit in a qubit–qutrit system, we are interested in t-designs formed by projectors of higher rank—namely rank three. Nevertheless, we will briefly first review the case of t-designs formed by rank-1 projection operators. In this case, quantum t-designs can be defined as sets of projectors $\{|\psi_j\rangle\langle\psi_j| ; j = 1, \ldots, N\}$ on the states $|\psi_j\rangle$ and corresponding weights $p_j > 0$ with $\sum_{j=1}^{N} p_j = 1$ which fulfill [54]

$$\sum_{j=1}^{N} p_j \, |\psi_j\rangle\langle\psi_j|^{\otimes t} = \int \mathrm{d}\psi \, |\psi\rangle\langle\psi|^{\otimes t} \tag{9}$$

where the integral is taken over a uniform distribution of all states of the Hilbert space. POVMs are 1-designs [55]. Examples of quantum 2-designs with equal weights, $p_j = 1/N$ for $j = 0, \ldots, N$, are SIC-POVMs [24] and complete sets of MUBs [56]. If complete sets of MUBs are not available, as is the case for dimension six, the construction of weighted 2-designs with non-equal weights can be useful [54]. Under the assumption of linear reconstruction, it has been shown that quantum 2-designs are ideal for QST performed by one repeated generalized measurement described by one informationally complete POVM [55] and for projective non-degenerate measurements [54].

In references [30, 57, 58], quantum t-designs of higher rank have been investigated and examples have been constructed. Appleby [58] has found quantum 2-designs of higher rank which behave similarly to SIC-POVMs, termed symmetric informationally complete measurements. The maximal orthoplex-bound-achieving sets of half-dimensional subspaces discussed above are examples of higher-rank $(n/2)$ quantum 2-designs [30, 57]. It was first considered by Zauner [57] as an example of a quantum 2-design consisting of operators of higher rank. Bodmann and Haas [30] explicitly construct these 2-designs using complete sets of MUBs and Johnson codes.

6. Methods

6.1. Formulation of the optimization problem

The QST quorum for a qubit–qutrit system consists of 35 measurements each described by a projector on a three-dimensional subspace of the six-dimensional Hilbert space. In order to parametrize the projectors, we use three pairwise orthogonal vectors of the Hilbert space. By vectors we mean here normalized vectors with arbitrary global phase. In general, such a vector in $\mathbb{C}^6$ is given by ten real parameters. However, we can choose each of the three vectors effectively in a four-dimensional Hilbert space. The reason is the dimensionality of the involved spaces: for any three-dimensional subspace and any four-dimensional subspace of a six-dimensional Hilbert space there is at least one vector which is a common element of both subspaces. If we have chosen the first vector of our three-dimensional subspace in this way, we can choose the second vector from a four-dimensional subspace of the five-dimensional space which is orthogonal on the first vector. Analogously, any two-dimensional subspace and any four-dimensional subspace of a five-dimensional Hilbert space have at least one vector in common. Finally, the third vector is chosen from the remaining four-dimensional subspace orthogonal on the first and the second vector. Each of the vectors,

denoted in a basis of the respective four-dimensional subspace by $|\psi\rangle = \sum_{i=1}^{4} x_i |i\rangle$, is given by six real parameters, $\theta_1, \theta_2, \theta_3$ and $\varphi_2, \varphi_3, \varphi_4$, in the following way,

$$x_1 = \cos\ \theta_1, \tag{10}$$

$$x_2 = \sin\ \theta_1\ \cos\ \theta_2\ e^{i\varphi_2}, \tag{11}$$

$$x_3 = \sin\ \theta_1\ \sin\ \theta_2\ \cos\theta_3\ e^{i\varphi_3}, \tag{12}$$

$$x_4 = \sin\ \theta_1\ \sin\ \theta_2\ \sin\theta_3\ e^{i\varphi_4}. \tag{13}$$

We compute a unitary operation which maps the second vector into the space orthogonal to the first. Then we compute a unitary operation which maps the third vector on the space orthogonal to the first and the second vector. Thus, each projector is given by 18 real parameters. Furthermore, we know that the quorum performance is invariant under any unitary operation on the Hilbert space. Therefore, we can choose for the first projector without loss of generality, $P_1 = \mathrm{diag}(1, 1, 1, 0, 0, 0)$, i.e. that it projects on the first three basis states for whatever basis we have chosen. Overall, our optimization problem has $N_{\mathrm{params}} = 34 \times 3 \times 6 = 612$ real parameters.

6.2. Numerical approaches

The goal of this section is to describe the numerical methods used, and to provide sufficient technical details of packages, function implementations, and parameters used, in order to allow for reproducibility of the results.

6.2.1. Maximizing the volume spanned by the traceless parts of the projection operators

The set of traceless parts, $\{Q_1, \ldots, Q_{n^2-1}\}$ of the projectors forming the QST quorum can be written in a $(n^2 - 1) \times (n^2 - 1)$ matrix using an orthogonal basis for the space of traceless Hermitian $n \times n$ matrices. Then the quality measure $\mathcal{Q}$ is the determinant of this matrix. The objective of our optimization problem is to maximize the value of $\mathcal{Q}$.

6.2.2. Minimizing the non-orthogonal contribution

Coming close to the upper bound for the quality measure, $\mathcal{Q}_{\mathrm{ub}} = (3/2)^{35/2}$, see equation (6), we conjecture that $\mathcal{Q}_{\mathrm{ub}}$ can indeed be reached. In the following we can make use of this conjecture because then a quorum which reaches the maximum for the geometric quality measure also has no non-orthogonal contributions for the matrices $Q_1, \ldots, Q_{35}$. To deal with slow convergence, we additionally consider a measure of non-orthogonality,

$$L = \sum_{i \neq j} |\mathrm{tr}(Q_i^{\dagger} Q_j)|, \tag{14}$$

where $i, j \in \{1, \ldots, 35\}$. Details of the optimization procedure including maximizing $\mathcal{Q}$ and $\ln(L)$ are provided in section 6.2.4 below.

In figure 3(a) we demonstrate the relationship between projectors' parameter values and the quality measure $\mathcal{Q}$. In figure 3(b) we show the relationship between the parameter values, describing the projection operators and the non-orthogonal contribution of the traceless parts of the projectors for the same two parameters. For simplicity of the visual representation, all parameters here are optimized, except for parameters 611, 612. These two parameters give the phases φ_4, see equation (13), for the third vector spanning the 34th and the 35th subspace, and are denoted by $\varphi_4^{34,3}$ and $\varphi_4^{35,3}$. The two plots show the respective search spaces of the two aforementioned optimization objectives. We explore the search spaces to look for the optimum. The global optimum coincides for both objectives, it maximizes the volume spanned by the projection operators, as well as the traceless parts of the projection operators in the optimal quorum are orthogonal. The numerically optimized values used for the plot are available as supplemental material at [59].

6.2.3. Powell's local search

In order to numerically optimize the set of measurement operators, we used a local search method (Powell's derivative-free method [45]) suitable for finding local optima in continuous optimization problems. The optimization problem is non-convex with many local optima, which is why the local search approach was used with different starting points in parallel to assure diverse exploration of the search space.

Powell's derivative-free method is useful for calculating the local minimum of a continuous but complicated function, where it is not trivial to take a derivative. Powell's method is known to perform very well as a local optimizer. Two of us applied it successfully to another QST optimization problem [29]. By starting it with 1000 diverse and different starting points we explore (and exploit) the search space well.

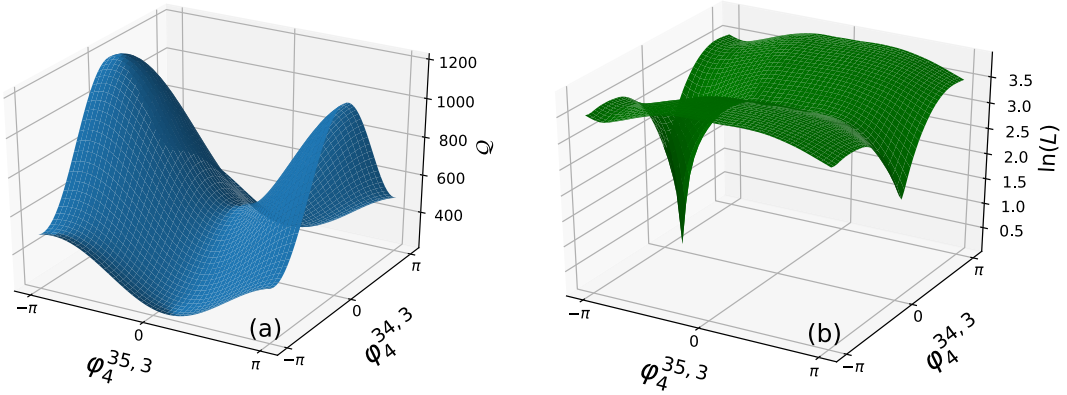

Figure 3. Optimization search in the landscape of potential solutions. For simplicity of the visual representation, all parameters are optimized, except for parameters that give the phases φ_4, see equation (13), for the third vector spanning the 34th and the 35th subspace. Therefore, they are denoted by $\varphi_4^{34,3}$ and $\varphi_4^{35,3}$.

Table 1. Parameters for the minimize function applied to minimize $-\mathcal{Q}$ and $\ln(L)$. The first column gives the number the *minimize* function is applied.

# Minimize	xtol	ftol	Maxiter
1–104	10^{-4}	10^{-4}	6.12×10^5
105–144	10^{-6}	10^{-6}	6.12×10^5
145–159	10^{-7}	10^{-7}	6.12×10^5
159–164	10^{-8}	10^{-8}	6.12×10^5
165–169	10^{-8}	10^{-8}	10^6
169–172	10^{-8}	10^{-8}	10^7
173–182	10^{-8}	10^{-8}	10^6
183–242	10^{-8}	10^{-8}	10^5
242–512	10^{-8}	10^{-8}	10^4

6.2.4. Technical details

Using Powell's local search method, we alternated between maximizing the volume spanned, and minimizing $\ln(L)$ for 512 iterations. We start this alternation procedure with using the standard parameters for the *minimize* function in the scipy package for python. For the sake of reproducibility, we provide the parameters of the *minimize* function in table 1.

6.3. Construction of the maximal orthoplex set from the optimal set of projectors

Finally, we use the optimal set of 35 projectors to construct a maximal orthoplex set of 70 projectors, by using the method described in [30]. Namely, for each of the projectors in the optimal set, we add its orthogonal complement. The construction of the maximal orthoplex set in such a way is made possible by the fact that the traceless parts of the 35 projectors in the optimal set are (approximately) pairwise orthogonal, $\mathrm{tr}(Q_i^\dagger Q_j) \approx 0$ for $j \neq j$.

7. Numerical results

The best result we obtained numerically for the geometric quality measure is

$$\mathcal{Q}_{\mathrm{num}} = 1206.53, \tag{15}$$

which corresponds to a deviation of $\Delta\mathcal{Q}/\mathcal{Q}_{\mathrm{ub}} = (\mathcal{Q}_{\mathrm{ub}} - \mathcal{Q}_{\mathrm{num}})/\mathcal{Q}_{\mathrm{ub}} = 1.3 \times 10^{-4}$. For the following measure of non-orthogonality, L this quorum yields $\ln(L) = -0.083\,94$. We include the corresponding parameters which determine the rank-3 projection operators of the quorum as well as the implementation of the computation of the quality measure $\mathcal{Q}_{\mathrm{num}}$ and of $\ln(L)$ from these parameters in supplemental materials available at [59].

Certainly, coming close to the upper bound for the geometric quality measure is not a proof of the existence of a quorum which actually achieves the upper bound. However, for practical purposes, the small deviation of our numerical result from the upper bound is inconsequential for the following reasons. The average information gain $\langle\mathcal{I}\rangle$, quality measure $\mathcal{Q}$, and number of repetitions of each of the measurements, N_{rep} obey the relation given in equation (3), see section 2. This relation yields

$$N_{\mathrm{rep}} \sim \mathcal{Q}^{-2/(n^2-1)}. \tag{16}$$

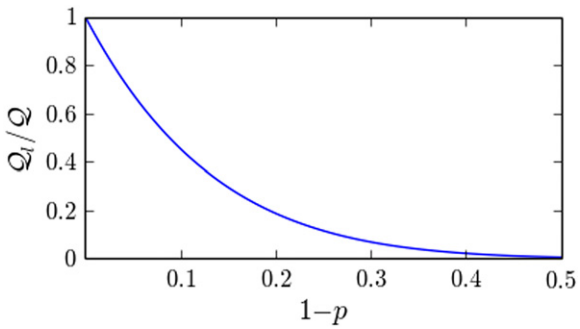

Figure 4. Loss-affected quality measure $\mathcal{Q}_l$ as a function of the probability $1-p$ that a quantum state is lost.

Here ($n = 6$), the relative deviation of 1.3×10^{-4} for the quality measure corresponds to a necessary relative increase in the number of repetitions of merely 10^{-5}. This implies that if $N_{\text{rep}} = 10^5$ for the ideal quorum, the deviation in quality of our quorum can be compensated by just one more repetition of each of the measurement.

The relation equation (16) also allows to take loss into account. For simplicity, we consider here the case where each of the measurement is subject to loss at the same rate. This is justified if the loss happens during the elementary measurements while the unitary operations are free of loss. Let us assume that for each experimental run, with a probability p the measurement is performed as intended and with a probability $1-p$ the quantum state is lost and there is no measurement result. This can be compensated by increasing the numbers of repetitions by a factor of $1/p$. To take this into account, a loss-affected quality measure $\mathcal{Q}_l$ is given by $\mathcal{Q}_l = \mathcal{Q}p^{(n^2-1)/2}$, see figure 4.

8. Discussion

In this paper, we have optimized a QST scheme for a qubit–qutrit system where only the qubit can be measured directly and all unitary operations are available. The quality of our solution approximates the upper bound which corresponds to the situation where the measurements project onto subspaces which are mutually unbiased. For practical purposes, the disadvantage of not fully achieving the upper bound can be disregarded. From a mathematical perspective, however, the explicit construction of a set of 35 mutually unbiased three-dimensional subspaces in $\mathbb{C}^6$ remains an open problem. Such a construction might also allow a generalization to higher composite dimensions such as ten or twelve, where the numerical approach is significantly more difficult than for the six-dimensional case studied in this paper. While this example of a qubit–qutrit system is of importance in its own right given its realization by an NV center, our general approach can be applied to a broad range of QST problems under limited measurements. This might allow experimentalists to find the most optimal QST scheme for their specific system.

Our method of numerically solving the smaller-dimensional problem of finding a set of projection operators, optimal for QST in the sense of [21], and then extending this set to build a maximal set which approximates the orthoplex bound may be employed for looking for approximations of maximal orthoplex-bound-achieving sets in higher dimensions.

For a higher dimension $n > 6$, the optimization problem becomes computationally more challenging. Further future research might include the application and tailoring of machine learning methods to the high-dimensional optimization problem. In reference [60], we have already applied machine learning methods and obtained rank-1 QST quorums in dimension eight which are improved compared to the result achieved by standard numerical methods used in [29].

Acknowledgments

This work was partially supported by the Zukunftskolleg (University of Konstanz) and the Bulgarian National Science Fund under the Contract No. KP-06-M32/8.

Author contributions

VNI-R and NR developed the idea of customized QST and implemented the numerics for the rank-3 projectors in dimension six. GB identified and discussed the example for a qubit–qutrit system. All authors participated in the discussion of the results and in writing the manuscript.

Data availability statement

The parameters for the best quorum we have found as well as a python program which computes the geometric quality measure $\mathcal{Q}$ and the logarithm of the non-orthogonality measure, $\ln(L)$ are available online [59].

ORCID iDs

Guido Burkard https://orcid.org/0000-0001-9053-2200
Niklas Rohling https://orcid.org/0000-0002-2067-5852

References

[1] Shor P W 1997 Polynomial-time algorithms for prime factorization and discrete logarithms on a quantum computer *SIAM J. Comput.* **26** 1484
[2] Georgescu I M, Ashhab S and Nori F 2014 Quantum simulation *Rev. Mod. Phys.* **86** 153
[3] Bruzewicz C D, Chiaverini J, McConnell R and Sage J M 2019 Trapped-ion quantum computing: progress and challenges *Appl. Phys. Rev.* **6** 021314
[4] Arute F *et al* 2019 Quantum supremacy using a programmable superconducting processor *Nature* **574** 505
[5] Kjaergaard M, Schwartz M E, Braumüller J, Krantz P, Wang J I-J, Gustavsson S and Oliver W D 2020 Superconducting qubits: current state of play *Annu. Rev. Condens. Matter Phys.* **11** 369
[6] Loss D and DiVincenzo D P 1998 Quantum computation with quantum dots *Phys. Rev.* A **57** 120
[7] Kloeffel C and Loss D 2013 Prospects for spin-based quantum computing in quantum dots *Annu. Rev. Condens. Matter Phys.* **4** 51
[8] Nizovtsev A P, Kilin S Y, Jelezko F, Gaebal T, Popa I, Gruber A and Wrachtrup J 2005 A quantum computer based on NV centers in diamond: optically detected nutations of single electron and nuclear spins *Opt. Spectrosc.* **99** 233
[9] Altepeter J B, James D F and Kwiat P G 2004 Qubit quantum state tomography *Quantum State Estimation* (*Lecture Notes in Physics* vol 649) ed M Paris and J Řeháček (Berlin: Springer)
[10] Emerson J, Alicki R and Życzkowski K 2005 Scalable noise estimation with random unitary operators *J. Opt. B: Quantum Semiclass. Opt.* **7** S347
[11] Mavadia S, Edmunds C L, Hempel C, Ball H, Roy F, Stace T M and Biercuk M J 2018 Experimental quantum verification in the presence of temporally correlated noise *npj Quantum Inf.* **4** 7
[12] Merkel S T, Gambetta J M, Smolin J A, Poletto S, Córcoles A D, Johnson B R, Ryan C A and Steffen M 2013 Self-consistent quantum process tomography *Phys. Rev.* A **87** 062119
[13] Blume-Kohout R, Gamble J K, Nielsen E, Mizrahi J, Sterk J D and Maunz P 2013 Robust, self-consistent, closed-form tomography of quantum logic gates on a trapped ion qubit (arXiv:1310.4492)
[14] Nielsen E, Gamble J K, Rudinger K, Scholten T, Young K and Blume-Kohout R 2020 Gate set tomography (arXiv:2009.07301)
[15] Nielsen M A and Chuang I L 2010 *Quantum Computation and Quantum Information* 2nd edn (Cambridge: Cambridge University Press) ch 8
[16] Altepeter J B, Branning D, Jeffrey E, Wei T C, Kwiat P G, Thew R T, O'Brien J L, Nielsen M A and White A G 2003 Ancilla-assisted quantum process tomography *Phys. Rev. Lett.* **90** 193601
[17] Leung D W 2003 Choi's proof as a recipe for quantum process tomography *J. Math. Phys.* **44** 528
[18] Tóth G, Wieczorek W, Gross D, Krischek R, Schwemmer C and Weinfurter H 2010 Permutationally invariant quantum tomography *Phys. Rev. Lett.* **105** 250403
[19] Flammia S T, Gross D, Liu Y-K and Eisert J 2012 Quantum tomography via compressed sensing: error bounds, sample complexity and efficient estimators *New J. Phys.* **14** 095022
[20] Kimmel S, da Silva M P, Ryan C A, Johnson B R and Ohki T 2014 Robust extraction of tomographic information via randomized benchmarking *Phys. Rev.* X **4** 011050
[21] Wootters W K and Fields B D 1989 Optimal state-determination by mutually unbiased measurements *Ann. Phys.* **191** 363
[22] de Burgh M D, Langford N K, Doherty A C and Gilchrist A 2008 Choice of measurement sets in qubit tomography *Phys. Rev.* A **78** 052122
[23] Řeháček J, Englert B-G and Kaszlikowski D 2004 Minimal qubit tomography *Phys. Rev.* A **70** 052321
[24] Renes J M, Blume-Kohout R, Scott A J and Caves C M 2004 Symmetric informationally complete quantum measurements *J. Math. Phys.* **45** 2171
[25] Huszár F and Houlsby N M T 2012 Adaptive Bayesian quantum tomography *Phys. Rev.* A **85** 052120
[26] Straupe S S 2016 Adaptive quantum tomography *JETP Lett.* **104** 510
[27] Granade C, Ferrie C and Flammia S T 2017 Practical adaptive quantum tomography *New J. Phys.* **19** 113017
[28] Rohling N and Burkard G 2013 Tomography scheme for two spin-1/2 qubits in a double quantum dot *Phys. Rev.* B **88** 085402
[29] Ivanova-Rohling V N and Rohling N 2019 Optimal choice of state tomography quorum formed by projection operators *Phys. Rev.* A **100** 032332
[30] Bodmann B G and Haas J I 2018 Maximal orthoplectic fusion frames from mutually unbiased bases and block designs *Proc. Am. Math. Soc.* **146** 2601
[31] Conway J H, Hardin R H and Sloane N J A 1996 Packing lines, planes, etc: packings in Grassmannian spaces *Exp. Math.* **5** 139
[32] Shor P W and Sloane N J A 1998 A family of optimal packings in Grassmannian manifolds *J. Algebr. Comb.* **7** 157
[33] Calderbank A R, Hardin R H, Rains E M, Shor P W and Sloane N J A 1999 A group-theoretic framework for the construction of packings in Grassmannian spaces *J. Algebr. Comb.* **9** 129
[34] Dhillon I S, Heath J R W Jr, Strohmer T and Tropp J A 2008 Constructing packings in Grassmannian manifolds via alternating projection *Exp. Math.* **17** 9
[35] Bodmann B G and Haas J 2016 Achieving the orthoplex bound and constructing weighted complex projective 2-designs with Singer sets *Linear Algebr. Appl.* **511** 54

[36] Kocák T and Niepel M 2017 Families of optimal packings in real and complex Grassmannian spaces *J. Algebr. Comb.* **45** 129
[37] Zhang T and Ge G 2018 Combinatorial constructions of packings in Grassmannian spaces *Des. Codes Cryptogr.* **86** 803
[38] Casazza P G, Haas J I, Stueck J and Tran T T 2018 Constructions and properties of optimally spread subspace packings via symmetric and affine block designs and mutually unbiased bases (arXiv:1806.03549)
[39] Jasper J, King E J and Mixon D G 2019 Game of Sloanes: best known packings in complex projective space *Proc. SPIE 11138, Wavelets and Sparsity XVIII* p 111381E
[40] Casazza P G, Haas J I, Stueck J and Tran T T 2019 A notion of optimal packings of subspaces with mixed-rank and solutions (arXiv:1911.05613)
[41] Zheng L and Tse D N C 2002 Communication on the Grassmann manifold: a geometric approach to the noncoherent multiple-antenna channel *IEEE Trans. Inf. Theory* **48** 359
[42] Strohmer T and Heath R W 2003 Grassmannian frames with applications to coding and communication *Appl. Comput. Harmon. Anal.* **14** 257
[43] Love D J, Heath R W and Strohmer T 2003 Grassmannian beamforming for multiple-input multiple-output wireless systems *IEEE Trans. Inf. Theory* **49** 2735
[44] Yap D A, Roberts N and Prabhu V U 2019 Grassmannian packings in neural networks: learning with maximal subspace packings for diversity and anti-sparsity (arXiv:1911.07418)
[45] Powell M J D 1964 An efficient method for finding the minimum of a function of several variables without calculating derivatives *Comput. J.* **7** 155
[46] Seedhouse A *et al* 2020 Pauli blockade in silicon quantum dots with spin-orbit control (arXiv:2004.07078)
[47] Leon R C C *et al* 2020 Bell-state tomography in a silicon many-electron artificial molecule (arXiv:2008.03968)
[48] Childress L and Hanson R 2013 Diamond NV centers for quantum computing and quantum networks *MRS Bull.* **38** 134
[49] Awschalom D D, Hanson R, Wrachtrup J and Zhou B B 2018 Quantum technologies with optically interfaced solid-state spins *Nat. Photon.* **12** 516
[50] Dutt M V G, Childress L, Jiang L, Togan E, Maze J, Jelezko F, Zibrov A S, Hemmer P R and Lukin M D 2007 Quantum register based on individual electronic and nuclear spin qubits in diamond *Science* **316** 1312
[51] Neumann P, Beck J, Steiner M, Rempp F, Fedder H, Hemmer P R, Wrachtrup J and Jelezko F 2010 Single-shot readout of a single nuclear spin *Science* **329** 542
[52] Robledo L, Childress L, Bernien H, Hensen B, Alkemade P F A and Hanson R 2011 High-fidelity projective read-out of a solid-state spin quantum register *Nature* **477** 574
[53] Bodmann B and Haas J 2020 A short history of frames and quantum designs *Topological Phases of Matter and Quantum Computation* (*Contemporary Mathematics* vol 747) ed P Bruillard, C Ortiz Marrero and J Plavnik (Providence, RI: American Mathematical Society) p 215
[54] Roy A and Scott A J 2007 Weighted complex projective 2-designs from bases: optimal state determination by orthogonal measurements *J. Math. Phys.* **48** 072110
[55] Scott A J 2006 Tight informationally complete quantum measurements *J. Phys. A: Math. Gen.* **39** 13507
[56] Klappenecker A and Rötteler M 2005 Mutually unbiased bases are complex projective 2-designs *Proc. Int. Symp. on Information Theory* pp 1740–4
[57] Zauner G 1999 Quantendesigns: Grundzüge einer nichtkommutativen Designtheorie *PhD Thesis* University of Vienna
Zauner G 2011 Quantum designs: foundations of a non-commutative design theory *Int. J. Quantum Inf.* **9** 445 (Engl. transl.)
[58] Appleby D M 2007 Symmetric informationally complete measurements of arbitrary rank *Opt. Spectrosc.* **103** 416
[59] Supplemental material, available under https://doi.org/10.5281/zenodo.4304007
[60] Ivanova-Rohling V N and Rohling N 2020 Evaluating machine learning approaches for discovering optimal sets of projection operators for quantum state tomography of qubit systems *Cybern. Inf. Technol.* **20** 61